Proceedings of the 2004 IEEE
International Conference on Robotics & Automation
New Orleans, LA • April 2004

Energy-Based Control of a Passive Haptic Device

Changhyun Cho
Dept. of Mechanical Eng., Korea Univ.
Intelligent Robotics Res. Center, KIST
Seoul, Korea
chcho@kist.re.kr

Jae-Bok Song
Dept. of Mechanical Eng.
University of Korea
Seoul, Korea
jbsong@korea.ac.kr

Munsang Kim & Chang-Soon Hwang
Intelligent Robotics Res. Center
KIST
Seoul, Korea
{munsang & cshwang}@kist.re.kr

***Abstract* - In this paper, we propose an energy-based control method of a passive haptic device equipped with electric brakes. Unstable behavior is observed in the passive haptic system due to time delay mainly arising from the slow update rate of the virtual environment. From the passive FME (Force Manipulability Ellipsoid) analysis, a so-called direct force control method is proposed in this paper. Its gain is computed by force analysis at the end-effector of a passive haptic device so that the component of a resultant force at the end-effector causing a pullback motion becomes zero. However, this direct force control scheme requires precise measurement of the hand force input by a human operator. We also propose the indirect force control scheme in which the gain in the direct force control scheme is computed using the notion of passivity without resorting to the high precision force sensor. For the experiments a 2-link passive haptic system was developed in this research. Various experiments have been conducted to investigate the validity of both direct and indirect force control schemes proposed in this paper. It is shown that both schemes produce satisfactory performance in the force display for the wall-following task on the virtual wall.**

Index Terms* - *direct force control, indirect force control, passive haptic device, passivity.

I. INTRODUCTION

A passive actuator such as a brake is stable and has an advantage of a good torque/mass ratio. However, it has a very serious limitation in generating its braking torque: passive actuators can generate a torque only against direction of its motion. Due to this inability of a passive actuator, a desired force can be displayed only approximately in some regions. *Force approximation* applied to a passive haptic device is inevitable and is frequently used specially on the wall-following task in that the human operator wants to move the end-effector along the surface of a virtual wall. During the wall-following task, *unsmooth motion* (i.e., contact and non-contact of the end-effector with a virtual wall) is often observed. Colgate noted that force approximation causes such an unsmooth motion [1]. Several control algorithms have been suggested to avoid this type of unsmooth force display.

Swanson and Book presented the single degree of freedom controller (SDOF controller), which used the SDOF line achieved by locking one brake to reduce a system DOF [2]. They also suggested an optimal control concept on the proposed velocity ratio controller which was applied to a velocity field [3]. Cost functions were constructed to minimize approximation angle and kinetic energy loss. Sakaguchi et al. proposed a small band set up near the surface to move along the surface of a virtual wall [4]. Only one brake was activated in the small band as in the SDOF controller in [2].

In spite of the features of unsmooth motion similar to the unstable motion of an active haptic device, however, no one has dealt with the issue of unsmooth motion from the viewpoint of stability. Like an active haptic system, a passive one also involves the problem of time delay due to the slow update rate of VE. From the passive FME (Force Manipulability Ellipsoid) analysis [5], it was observed that a passive haptic system with time delay shows unstable behavior (i.e., unsmooth motion), when a passive haptic device obtains the pullback capability due to force approximation. The *pullback capability*, which would be available only in active actuators, enables the end-effector to leave the wall surface by a resultant force at the end-effector.

From the analysis of the force distribution at the end-effector readily provided by the passive FME, the brake torques can be controlled such that the unsmooth force display due to the pullback motion can be eliminated during the wall-following task. However, this control scheme requires a high precision force/torque sensor to accurately measure the force applied by a human operator. In this paper, a passivity-based control method is proposed to control the brakes for smooth force display without the use of a high-precision force/torque sensor. The time-domain passivity control method [6, 7] was extended to a passive system. It can be shown that smooth display can be achieved for the wall-following task with the proposed energy-based control method.

The rest of this paper is organized as follows. The passive FME is briefly introduced in Section 2, and the unsmooth behavior of a passive haptic device is discussed in Section 3. New force control schemes are proposed in Section 4. Section 5 deals with the 2 DOF coupled tendon-drive mechanism which was developed for experimental verification of the proposed control method and shows experimental results. Conclusions are drawn and future work is outlined in Section 6.

IV. PASSIVE FME (FORCE MANIPULABILITY ELLIPSOID)

In an electric brake, only the magnitude of a braking torque can be controlled, since the change in the polarity of the electromagnet does not affect its direction. A brake can generate its braking torque only in the passive region in which $\tau \cdot \dot{q} \le 0$ is satisfied, where $\dot{q}$ is the joint velocity. Therefore, if the brake is commanded to generate a desired torque τ_d in the active region (i.e., $\tau \cdot \dot{q} > 0$), the brake control torque τ_c

should be set to zero since the brake cannot produce τ_d. Taking this control feature into account, one can obtain the brake control torque by adopting the Karnopp's stick-slip model [8] as follows:

Slip mode ($\dot{q} \neq 0$)

$$\tau_c = \begin{cases} -\text{sgn}(\dot{q})|\tau_d| & \text{if } \text{sgn}(\dot{q}) \neq \text{sgn}(\tau_d) \\ 0 & \text{else} \end{cases} \quad (1a)$$

Stick mode ($\dot{q} = 0$)

$$\tau_c = \begin{cases} -\tau_h & \text{if } \text{sgn}(\tau_h) \neq \text{sgn}(\tau_d) \\ 0 & \text{else} \end{cases} \quad (1b)$$

where τ_h is the external torque acting on the brake shaft (e.g., the hand torque input applied by a human operator in most haptic devices). In what follows, (1) will be referred to as the *passive constraint*.

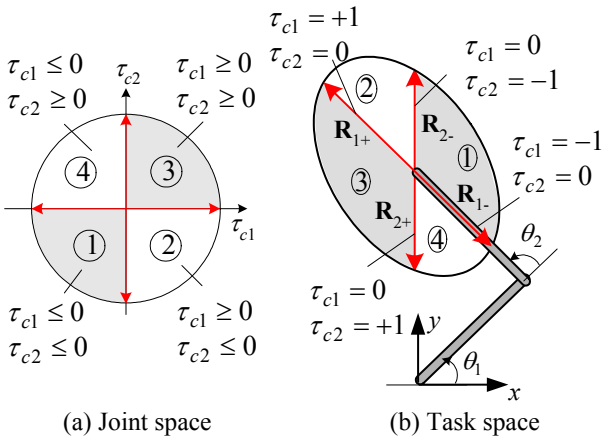

(a) Joint space (b) Task space

Fig. 1. A set of passive FMEs ($\theta_1 = 45°$, $\theta_2 = 90°$, $l_1 = l_2 = l$).

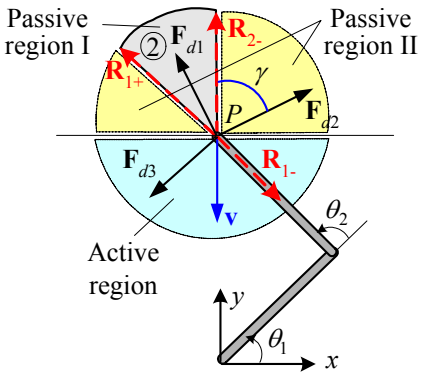

Fig. 2. Force approximation ($\theta_1 = 45°$, $\theta_2 = 90°$, $l_1 = l_2 = l$).

From all possible combinations of joint velocities and the hand torque inputs, it is observed in the 2 DOF mechanism that control torques can be represented by 4 regions as shown in Fig. 1(a), regardless of whether the joints are in either the slip mode or the stick mode. A set of passive FMEs can be drawn by mapping $\boldsymbol{\tau}_c$ in joint space into the end-effector force $\mathbf{F}_c$ in task space using the Jacobian mapping (i.e., $\boldsymbol{\tau} = \mathbf{J}(\mathbf{q})^T\mathbf{F}$). Thus each region in Fig. 1(a) is mapped into each corresponding passive FME illustrated in Fig. 1(b) which represents a set of passive FMEs. Each passive FME is delimited by four reference forces $\mathbf{R}_{1+}$, $\mathbf{R}_{1-}$, $\mathbf{R}_{2+}$, and $\mathbf{R}_{2-}$, where $\mathbf{R}_i$ denotes the end-effector force when only brake i is applied (i.e., $\tau_{ci} \neq 0$) with the other brakes released. For example, if $\tau_{c1} > 0$ (or $\tau_{c1} < 0$) with $\tau_{c2} = 0$, then force $\mathbf{R}_{1+}$ (or $\mathbf{R}_{1-}$) is generated.

Consider an example in Fig. 2 for detailed analysis. Suppose that the end-effector P is moving in the $-y$ direction (i.e., $\dot{\theta}_1 < 0$ and $\dot{\theta}_2 > 0$). Hence, the brakes can generate a force only in passive FME 2 (i.e., $\tau_{c1} > 0$ and $\tau_{c2} < 0$) because of the passive constraint. The desired force $\mathbf{F}_{d1}$ in this region (passive region I in Fig. 2) can be accurately displayed by a resultant force of $\mathbf{R}_{1+}$ and $\mathbf{R}_{2-}$. On the other hand, the desired $\mathbf{F}_{d2}$ needs to be represented by a combined force of $\mathbf{R}_{2-}$ and $\mathbf{R}_{1-}$ in Fig. 2. However generation of $\mathbf{R}_{1-}$ requires $\tau_{c1} < 0$ which violates the passive constraint of $\tau_{c1} \cdot \dot{\theta}_1 \le 0$. Therefore, $\mathbf{F}_{d2}$ (in passive region II) cannot be accurately displayed but approximately done by the nearest available force $\mathbf{R}_{2-}$ alone, which is called *force approximation* in passive haptic devices. It is convenient to define a force approximation angle γ between $\mathbf{R}_{2-}$ and $\mathbf{F}_{d2}$ as shown in Fig. 2, which represents a level of force approximation. Finally, the desired force $\mathbf{F}_{d3}$ cannot be displayed at all since it belongs to the active region of $\mathbf{F}\cdot\mathbf{v} > 0$. In the case of passive haptic devices, consequently, there exist regions in which the desired force cannot be displayed or can be displayed only approximately and these regions can be found by the passive FME analysis.

III. Unsmooth Behavior

Before dealing with a passive haptic device, consider unstable behavior of an active haptic device. The active haptic device can make the end-effector move toward the surface or even leave the wall surface using the active torque from the motor once it penetrates into the wall. This so-called pullback motion is beneficial to precisely representing the virtual environment (VE), but it easily leads to unstable behavior - repeated contact and non-contact with the wall – due to time delay mainly arising from the slow update rate of VE. On the ideal condition (i.e., no time delay), however, an active haptic device can display the wall smoothly. Also if it does not possess pullback capability, smooth display can be achieved regardless of time delay. Smooth display on the wall-following task by a passive haptic device can be also expected, since a passive haptic device cannot produce pullback motion. However, unsmooth motion frequently occurs during the wall-following task as in the active device.

In the next section, we will show how a passive haptic device is capable of pullback motion. First, the case in which no force approximation and smooth display are achieved

regardless of time delay is discussed. Second, pullback capability caused by force approximation is analyzed in detail.

A. *Force display without force approximation*

Consider the 2 DOF Cartesian manipulator shown in Fig. 3, where brakes 1 and 2 control the x-axis and y-axis movements, independently. Assume that the wall surface is frictionless. $\mathbf{F}_h$ denotes a hand force input given by a human operator, and F_{hx} and F_{hy} are its components in the x and y axes, respectively. The vector $\mathbf{n}$ is the surface normal vector in the $-y$ direction. Since the desired force $\mathbf{F}_d$ exactly matches the reference force $\mathbf{R}_{2-}$, it can be accurately displayed without force approximation with brake 2 alone.

Suppose that the end-effector moves along the y axis. As the penetration of the end-effector into the virtual wall increases, brake 2 also increases its braking force to the fully locked level. Then the penetration depth remains at a constant value during the wall-following task on the virtual wall with brake 2 locked, until the user pulls the end-effector back (i.e., the sign of F_{hy} changes). The end-effector can smoothly move due to free motion of joint 1 (i.e., with brake 1 released) on the x-axis while keeping the penetration depth constant. Time delay due to the slow VE update rate will not affect performance of force display in this ideal situation for the wall-following task.

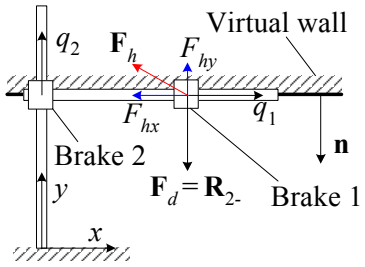

Fig. 3. X-Y table mechanism.

B. *Force display with force approximation*

If the virtual wall in Fig. 3 is slanted, then force approximation needs to be performed. The forces acting on the end-effector in this case are illustrated in Fig. 4 for different penetration depths which give different values of the desired force $\mathbf{F}_d$. The vectors $\mathbf{n}$ and $\mathbf{t}$ are the unit vectors normal and tangent to the virtual wall, respectively. Since the desired force $\mathbf{F}_d$ to display the wall should be normal to the wall surface, this force can be displayed only approximately by the nearest reference force $\mathbf{R}_{2-}$. The control force $\mathbf{F}_c$ generated by brake 2 and the hand force $\mathbf{F}_h$ given by the user act on the end-effector. Thus, $\mathbf{F}_r$, the resultant force of $\mathbf{F}_c$ and $\mathbf{F}_h$, is generated.

At the initial contact with the virtual wall, penetration depth is small, so $\|\mathbf{F}_{hc}\| > \|\mathbf{F}_c\|$ (i.e., case (a) in Fig. 4). Hence, the slip mode occurs at brake 2 and $\mathbf{F}_r$ has a normal component directed into the wall, thus resulting in increasing penetration. As penetration continues, the control force grows to reflect an increase in wall deflection until $\|\mathbf{F}_c\| = \|\mathbf{F}_{hc}\|$ (i.e., case (b)) is reached. In this case the normal component of the resultant force $\mathbf{F}_r$ is directed out of the wall, thereby moving the end-effector off the wall surface. In summary, even the passive haptic device can have pullback motion due to force approximation. This pullback motion causes the unsmooth motion during the wall-following task for the system with time delay (i.e., delayed virtual environment).

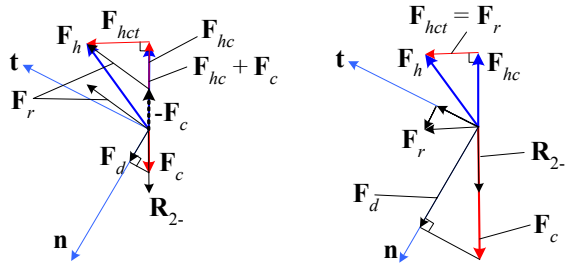

(a) Small penetration depth $\|\mathbf{F}_{hc}\| > \|\mathbf{F}_c\|$ (b) Large penetration depth $\|\mathbf{F}_{hc}\| \le \|\mathbf{F}_c\|$

Fig. 4. Forces acting on the end-effector under different penetration depths.

IV. Control Methods

In section III, we observed that fullback motion is possible in a passive haptic system due to force approximation. Because unsmooth force display is caused by this pullback motion, smooth display can be achieved regardless of the time delay by making the normal component of the resultant force $\mathbf{F}_r$ in Fig. 4(b) vanish. This underlying idea of the indirect force control scheme is proposed in this research.

A. *Direct force control method*

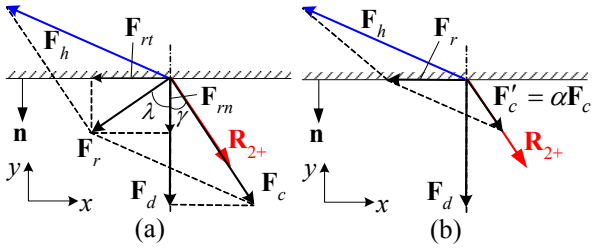

Fig. 5. Forces acting on the end-effector.

Fig. 5 illustrates the various forces involved in representing a virtual wall for the manipulator shown in Fig. 2. Proper brake control can be found by observing the relations of these forces. If the desired force $\mathbf{F}_d$ is to be displayed approximately by the reference force $\mathbf{R}_{2+}$, for example, then the control force $\mathbf{F}_c$ is generated in the direction of $\mathbf{R}_{2+}$ with an approximation angle γ between $\mathbf{F}_d$ and $\mathbf{F}_c$. The resultant $\mathbf{F}_r$ of all the forces acting on the end-effector becomes

$$\mathbf{F}_r = \mathbf{F}_{rn} + \mathbf{F}_{rt} = \mathbf{F}_h + \mathbf{F}_c \qquad (2)$$

where $\mathbf{F}_{rn}$ and $\mathbf{F}_{rt}$ are the normal and tangential components of $\mathbf{F}_r$. In Fig. 5(a), $\mathbf{F}_{rn}$ is directed out of the wall, thus moving the end-effector off the wall surface.

Because unsmooth wall-following is caused by repeated contact and non-contact of the end-effector with the wall, the proposed brake control attempts to make the normal component $\mathbf{F}_{rn}$ go to zero by adjusting the brake torques (e.g., reducing brake torques) as shown in Fig. 5(b). Then the end-effector becomes subject to only the tangential force along the surface; therefore, it can follow the wall smoothly without leaving the wall surface. A new control force $\mathbf{F}'_c$ is given by

$$\mathbf{F}'_c = \alpha \mathbf{F}_c \tag{3}$$

where α is the scale factor. Substitution of (3) into (2) yields

$$\mathbf{F}_h + \mathbf{F}'_c = \mathbf{F}_h + \alpha \mathbf{F}_c \tag{4}$$

Since $\mathbf{F}_r$ is normal to $\mathbf{F}_d$ with the new control force $\mathbf{F}'_c$, $(\mathbf{F}_h + \alpha\mathbf{F}_c) \cdot \mathbf{F}_d = 0$, and the following relation is obtained.

$$\alpha = -(\mathbf{F}_h \cdot \mathbf{F}_d)/(\mathbf{F}_c \cdot \mathbf{F}_d) \tag{5}$$

Let us investigate the sign of α. Only when $\mathbf{F}_h \cdot \mathbf{F}_d < 0$, the user intends to move the end-effector while maintaining it in contact with the wall; otherwise, the user intends to move the end-effector off the wall and thus force reflection is not necessary. On the other hand, only when $\mathbf{F}_c \cdot \mathbf{F}_d > 0$, the approximation angle γ between the desired and the reference force is less than 90^o and thus force approximation is possible. Consequently, $\alpha > 0$ since $\mathbf{F}_h \cdot \mathbf{F}_d < 0$ and $\mathbf{F}_c \cdot \mathbf{F}_d > 0$. Furthermore, the value of α is in the range of $0 < \alpha \leq 1$. Note that $\alpha > 1$ means that the brake is commanded to generate the torque greater than the desired torque, which is unreasonable.

Considering that a virtual wall generally has the bilateral characteristic, it is appropriate that α should be computed with (5) while the end-effector is inside the wall but moves outwardly. The outward motion can cause the unsmooth behavior as explained in the previous section. When the end-effector moves inwardly, brakes are firmly activated to retard the on-going penetration of the end-effector. Thus, α should be computed with (5), when $\mathbf{F}_d \cdot \mathbf{v} > 0$ (i.e., outward motion). This proposed scheme is called a *direct force control method* because the value of α can be determined directly from the passive FME.

B. *Indirect force control method*

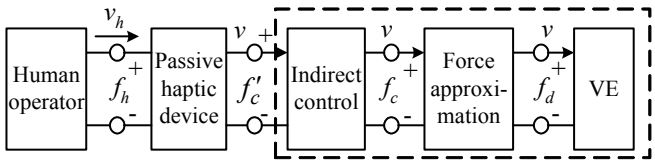

Fig. 6. Passive haptic interface system with delayed virtual environment.

Although α can be computed accurately from (5), this computation requires the precise measurement of $\mathbf{F}_h$, which is usually carried out by a high-cost force/torque sensor. Therefore, a passivity approach is proposed in this research to compute the scale factor α without resorting to the precise measurement of $\mathbf{F}_h$. Since α is computed indirectly by the passivity-based approach, the proposed control scheme will be referred to as the *indirect force control*.

The haptic interface in a passive haptic device is shown in Fig. 6. A human operator moves the end-effector at a velocity of v_h and the subsequent velocities are assumed to be equal to v_h. The force f_d is the desired force given by the physical laws in the VE (Virtual Environment), f_c is the control force modified from f_d inevitably by the force approximation process, and f'_c is the force computed by the indirect force control scheme. From (3), the indirect force control scheme is defined by

$$f'_c(k) = \alpha(k)\, f_c(k) \tag{6}$$

Since the unsmooth motion of a passive haptic device is caused by both time delay (due to the slow update rate of VE) and force approximation, computation of the passivity should take these active elements into account. A discrete form of passivity [7], $W(k)$, of the dashed area in Fig. 6 can be represented by

$$W(k) = \sum_{k=1}^{n} \alpha(k-1) f_c(k-1) v(k) T + W(0) \tag{7}$$

where $W(0)$ denotes the initial passivity, and T is the sampling period. Note that (7) is obtained by summing up the passivity at each port. It is also noted that the passivity at time k is computed from the force at time k-1 in (7), because one sampling period is required for force computation in VE.

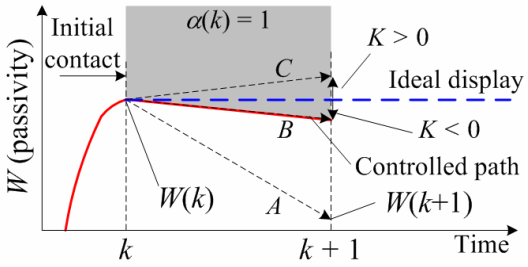

Fig. 7. Passivity plots as a function of time, showing the concept of passivity-based control.

The control objective is to regulate braking torques to imitate the ideal force display shown in Fig. 3. Passivity plots for both ideal and actual situation are illustrated in Fig. 7. In the ideal force display shown in Fig. 3, passivity does not change after the initial contact with the wall (i.e., $f'_c(k\text{-}1)\, v(k)\, T = 0$) because $v(k) = 0$ owing to no pullback capability of the passive device. However, if the pullback motion occurs due to force approximation, then $v(k)\, f_c(k) < 0$ and the passivity may steeply decrease as in path A in Fig. 7. If the situation continues, the unsmooth motion is likely to occur because the passivity becomes negative. In this case, path A should be shifted toward the ideal path by properly adjusting $\alpha(k)$.

To execute this control strategy, consider the predicted variation of passivity at time $k+1$ for the dashed area in Fig. 7. From (7), since $v(k+1)$ is not available at time k, the predicted variation of passivity is given by

$$\alpha(k) f_c(k) v(k) = K \tag{8}$$

where K is the predetermined constant used for computing $\alpha(k)$ $(= K/\{f_c(k)v(k)\})$. It is noted that K represents the variation of passivity during one sampling period T; $K > 0$ (or $K < 0$) denotes an increase (or decrease) in passivity. Note that the passivity increases as the penetration increases because $v(k) > 0$ and usually $f_c(k) > 0$ in Fig. 6. For the ideal display, $K = 0$ because $v(k) = 0$ owing to no pullback capability. Setting K to zero to imitate this ideal display leads to $\alpha(k) = 0$ (because usually $v(k)f_c(k) \neq 0$), thus resulting in fully releasing of all brakes. It is desirable, therefore, that K should be set to a small value for a nonzero value of $\alpha(k)$. Since Path C in Fig. 7 corresponding to a positive K increases the penetration of the end-effector, K should have a negative sign as in path B to avoid further penetration of the end-effector during the force control.

It is reasonable that α is computed from (8) only when the end-effector is inside the wall but moves outwardly (i.e., during the pullback motion) as investigated in the direct force control method. From these observation, $\alpha(k)$ can be computed by

$$\alpha(k) = \begin{cases} K/\{v(k) f_c(k)\} & \text{if } v(k) f_c(k) < K \\ 1 & \text{else} \end{cases} \tag{9}$$

where $K < 0$. Since $f_c(k)v(k) < K < 0$, $\alpha(k) > 0$. Consequently, $0 < \alpha(k) \leq 1$. Implementation of the indirect force control is summarized as follows:

1. Compute $f_c(k)$ according to the passive constraint.
2. Obtain $\alpha(k)$ from (9).
3. Find the modified force $f'_c(k) = \alpha(k) f_c(k)$.
4. Generate the brake torques to deliver $f'_c(k)$ using the Jacobian relation.

V. Experiments

A. Experimental setup

Various experiments have been conducted with a 2-link device equipped with 2 electric brakes as shown in Fig. 8. The FT (force/torque) sensor is mounted at the handle to measure the hand force provided by the user. Rotational motion of each brake is sensed by the optical encoder mounted on the brake axis. The brake control is conducted at a rate of 1kHz. Since the brake is capable of generating a braking torque proportional to the current input, it is controlled in an open-loop manner. The virtual wall is modeled as a spring whose constant is 10^7N/m, but is assumed to possess neither damping nor friction on the surface. Thus a desired force is directed in the surface normal $\mathbf{n}$, which is in the $-y$ direction.

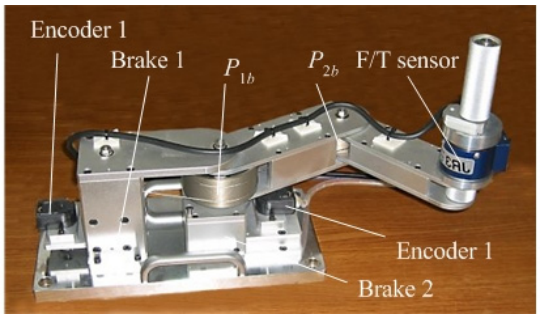

Fig. 8. Coupled tendon-drive mechanism.

B. Experimental results

The wall-following experiment was done on the virtual wall shown in Fig. 5 where the wall surface parallel to the x-axis is located at $y = 0.2$m. Only brake 2 was activated with brake 1 fully released during force display, so the control force $\mathbf{F}_c$ had the same direction as $\mathbf{R}_2$.. The approximation angle γ, an angle between the desired force and the control force as shown in Fig. 2, increased as the end-effector moves in the $+x$ direction. The minimum and maximum approximation angles were 3^o around $x = 0.06$m and 37^o around $x = 0.18$m, respectively.

The experimental results in Fig. 9 were obtained at the virtual wall update rate of 100Hz. Smooth paths of the end-effector were observed after the first contact for the direct and indirect force controls. The penetration depths also remained at a relatively constant value, whereas unsmooth motion (i.e., contact and non-contact) was repeated with no control (i.e., arrow markers in Fig. 9). We observed from the ω_{B2} plot that the duration of the stick mode was much shorter for both the force controls than for no control, thus indicating that brake 2 was not completely locked during the force controls. This can be reconfirmed by the plots of τ_{c2} and τ'_{c2}. Without force control (i.e., $\tau'_{c2} = \tau_{c2}$), τ_{c2} was set to the maximum value of 0.565Nm during the wall contact, so brake 2 was fully locked. However, τ'_{c2}'s computed by both the direct and indirect force control methods were not always saturated at the maximum value and showed the slip mode in brake 2. It was also noticed that F_{hy} changed gradually during force controls without sudden variations that frequently occurred without force control.

It is also noted that the tangential component of a hand force, F_{hx}, increases as the approximation angle γ increases. It means that a human operator feels a stronger force, which retards the motion along the surface as γ increases. This can be easily understood by investigating the forces acting on the end-effector as shown in Fig. 5. That is, the undesired force, $|\alpha \mathbf{F}_c|\sin\gamma$, due to force approximation increases with γ, but this value is less than the force $|\mathbf{F}_c|\sin\gamma$ for no control because $0 < \alpha \leq 1$. As a result, a human operator feels less retarding force along the surface with the proposed control scheme as shown in the enlarged plot of F_{hx}.

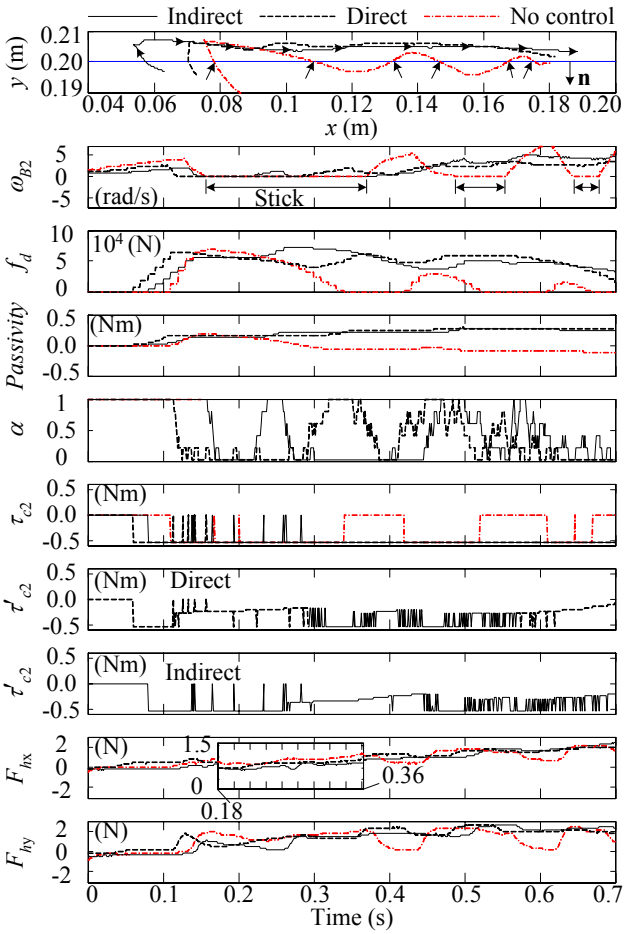

Fig. 9. Experimental results on a plane wall at the virtual wall update rate of 100Hz.

The system with no control sometimes exhibits unstable behavior (i.e., passivity < 0 as shown in the passivity plot in Fig. 9), whereas both the direct and indirect force control schemes show stable behavior for all time from the viewpoint of passivity. Passivity moderately increased with time during both the force controls in Fig. 9. Note that the indirect force control requires only the sign of the joint torques to compute (1b).

VI. Conclusions and Further Researches

From the passive FME analysis, it is observed that a passive haptic device with both time delay and force approximation shows poor (sometimes unstable) performance. Based on the passivity analysis, the indirect force control method has been developed to obtain the gain of the direct force control method in which the brake generates a torque so that the normal component of the resultant force acting on the end-effector becomes zero. Through various experiments, we have verified that the indirect force control method can improve performance of haptic display regardless of time delay. Moreover, it is shown that the indirect force control method produces the similar performance to the ideal display without any accurate force sensing required in implementation of the direct force control method. To increase performance of indirect force control, the accurate control of an electric brake should be available and a brake with faster response time is also necessary.

References

[1] J. E. Colgate, M. A. Peshkin and W. Wannasuphoprasit, "Nonholonomic Haptic Display," Proc. of the IEEE Int. Conf. on Robotics and Automation, pp. 539-544, April 1996.

[2] D. K. Swanson and W. J. Book, "Obstacle avoidance methods for a passive haptic display," Proc. of the IEEE Int. Conf. on Advanced Intelligent Mechatronics, pp.1187-1192, July 2001.

[3] D. K. Swanson and W. J. Book, "Path-following control for dissipative passive haptic displays," Proc. of 11th Symposium on Haptics, pp. 101-108, March 2003.

[4] M. Sakaguchi, J. Furusho and N. Takesue, "Passive force display using ER brakes and its control experiments," Proc. of Virtual Reality, pp.7-12, March 2001.

[5] C. H. Cho, M. S. Kim and J. B. Song, "Performance analysis of a 2-link haptic device with electric brakes," Proc. of 11th Symposium on Haptics, pp. 47 -53, March 2003.

[6] B. Hannaford and J. H. Ryu, "Time domain passivity control of haptic interfaces," IEEE Trans. On Robotics and Automation, vol. 18, no. 1, pp. 1-10, February 2002.

[7] J. H. Ryu, Y. S. Kim, and B. Hannaford, "Sampled and continuous time passivity and stability of virtual environments," Proc. of the IEEE Int. Conf. on Robotics and Automation, pp. 822-827, September 2003.

[8] D. Karnopp, "Computer simulation of stick-slip friction in mechanical dynamic system," ASME Journal of Dynamic Systems, Measurement, and Control, vol. 107, pp.100-103. March 1985.